

THE LAKE BAIKAL NEUTRINO EXPERIMENT: SELECTED RESULTS

V.A.BALKANOV^a, I.A.BELOLAPTIKOV^g, L.B.BEZRUKOV^a, N.M.BUDNEV^b, A.G.CHENSKY^b,
 I.A.DANILCHENKO^a, Zh.-A.M.DZHILKIBAEV^a, G.V.DOMOGATSKY^a, A.A.DOROSHENKO^a,
 S.V.FIALKOVSKY^d, O.N.GAPONENKO^a, A.A.GARUS^a, T.I.GRESS^b, D.KISSⁱ, A.I.KLIMOV^f,
 S.I.KLIMUSHIN^a, A.P.KOSHECHKIN^a, Vy.E.KUZNETZOV^a, V.F.KULEPOV^d, L.A.KUZMICHEV^c,
 S.V.LOVZOV^b, J.J.LAUDENSKAITE^b, B.K.LUBSANDORZHIEV^a, M.B.MILENIN^d, R.R.MIRGAZOV^b,
 N.I.MOSEIKO^c, V.A.NETIKOV^a, E.A.OSIPOVA^c, A.I.PANFILOV^a, Yu.V.PARFENOV^b, A.A.PAVLOV^b,
 E.N.PLISKOVSKEY^a, P.G.POKHIL^a, E.G.POPOVA^c, M.I.ROZANOV^e, I.A.SOKALSKI^a, CH.SPIERING^h,
 O.STREICHER^h, B.A.TARASHANSKY^b, G.TOHTⁱ, T.THON^h, R.VASILIEV^a, R.WISCHNEWSKI^h,
 I.V.YASHIN^c.

^a *Institute for Nuclear Research, Moscow, Russia*

^b *Irkutsk State University, Irkutsk, Russia*

^c *Institute of Nuclear Physics, MSU, Moscow, Russia*

^d *Nizhni Novgorod State Technical University, Nizhni Novgorod, Russia*

^e *St.Petersburg State Marine Technical University, St.Petersburg, Russia*

^f *Kurchatov Institute, Moscow, Russia*

^g *Joint Institute for Nuclear Research, Dubna, Russia*

^h *DESY-Zeuthen, Berlin/Zeuthen, Germany*

ⁱ *KFKI, Budapest, Hungary*

presented by G.V.Domogatsky

Institute for Nuclear Research, Moscow, Russia

E-mail: domogats@pcbai10.inr.ruhep.ru

ABSTRACT

We review the present status of the lake Baikal Neutrino Experiment and present selected physics results gained with the consecutive stages of the stepwise increasing detector: from NT-36 to NT-96. Results cover atmospheric muons, neutrino events, very high energy neutrinos, search for neutrino events from WIMP annihilation, search for magnetic monopoles and environmental studies. We also describe an air Cherenkov array developed for the study of angular resolution of NT-200.

1. Introduction

The Lake Baikal Neutrino Experiment exploits the deep water of the great Siberian lake as a detection medium for high energy neutrinos via muons and electrons, generated in high energy neutrino interactions. High energy neutrinos are of particular importance for high energy astrophysics for the last few decades to shed light on the physics of Active Galactic Nuclei (AGN), binary star systems, gamma ray burst (GRB) etc. The life time of the lake Baikal Neutrino Experiment spans almost two decades, from first small experiment with a few PMTs to the present large scale

neutrino telescope NT-200 ^{1,2,3)}, which has been put into full operation on April 6th 1998. The effective area of the telescope for muons is 2000-10000 m² depending on the muon energy. The expected rate of muons from atmospheric neutrinos, with a muon energy thresholds of 10 GeV and after all cuts rejecting background, is about 1 per two days.

2. Neutrino Telescope NT-200

2.1. Detector and Site

The Neutrino Telescope NT-200 is located in the southern part of Lake Baikal (51.50N and 104.20E) at 3,6km from the shore and at a depth of 1km. The absorption length L_{abs} of water at the site for wavelengths between 470nm and 500nm is about 20m and seasonal variations are less than 20%. The light scattering is subjected strongly to seasonal variations and from year to year. We can say now that light scattering is rather strongly anisotropic and typical values of L_{scatt} are about 15m. NT-200 (fig.1) consists of 192 optical modules (OMs) at 8 strings arranged at an umbrella like frame ^{1,2)}. Pairs of OMs are switched in coincidence with 15ns time window and define a channel. We pursue pairwise ideology for many reasons: to suppress individual OM background counting rates due to OM dark current and water luminescence, the level of late- and afterpulses etc. The OMs ⁴⁾ consists of QUASAR-370 phototube ^{5,6)} enclosed in transparent, nearly spherical pressure housing. The optical contact between the photocathode region of the phototube and the pressure sphere is made by liquid glycerine sealed with a layer of polyurethane. Apart from the phototube every OM contains two HV power supplies (25 kV and 2 kV), a voltage divider, two preamplifiers, a calibration LED and a vacuum probe. The QUASAR-370 phototube has been developed especially for the Lake Baikal Neutrino Experiment by INR and KATOD Company in Novosibirsk. The phototube is a hybrid one and has excellent time and amplitude resolutions.

The detector electronics system ²⁾ is hierarchical: from the lowest level to the highest one – OM's electronics, "sviazka" electronics module, string electronics module and the detector electronics module, where detector trigger signals are formed and all information from the string electronics module are received and sent to the shore station. The detector is operated from the shore station. A muon trigger is formed by the requirement of $\geq N$ hits (with hit referring to a channel) within 500 ns. N is typically set to the value 3 or 4. For such events, amplitude and time of all fired channels are digitized and sent to the shore. The event records includes all hits within a time window of -1000 ns to +800 ns with respect to the muon trigger signal. A separate monopole trigger system searches for clusters of sequential hits in individual channels which are characteristic for the passage of slowly moving, bright objects like GUT

monopoles.

There is a separate hydrological string to study permanently water parameters of the lake. This string is deployed at about 60m from the main part of NT-200.

There are two nitrogen lasers for the detector time calibration placed just above and below the detector. The former one illuminates each individual channel via fiber optics and the latter illuminates the detector as a whole.

2.2. Cherenkov EAS Array

To determine angular resolution of the NT-200 mobile wide angle air cherenkov array has been developed ⁷⁾. This array (Fig.2) has been deployed for the last two expeditions on the ice just above NT-200. It consists of four optical modules put on the sledges for fast deployment. Three of them are fixed in the vertices of an equilateral triangle and another one just in the center of the triangle. The sidelength of the triangle is about 100 m. The analog signals from the optical modules are fed by electrical coax cables to the central electronic station which is located near the central optical module. The data acquisition system includes 4 constant fraction discriminators, a majority coincidence unit, two TDCs with 500 ns and 5000 ns ranges, ADC, an EAS event counter, counting rate scalers for each channel and an underwater master signals counter.

Each optical module incorporates QUASAR-370G phototubes, two high voltage power supplies of 25 kV and 1 kV for an electron-optical preamplifier and small PMT respectively, anode pulses preamplifier and LED for amplitude calibration. The phototube is arranged into light tight metallic box which is equipped with mechanically removable lid. To increase the sensitivity area, Winston cones are used providing almost 2450 cm² final sensitive area by a factor of 2 larger than in the 1998 array. The angular acceptance of the optical module is restricted to 30^o of half angle. The QUASAR-370G phototube is practically the same as the phototube used in NT-200 but with six stages small PMT developed to withstand high mean anode current due to night sky background (NSB). To stabilize the phototubes gain, the HV power supplies are surrounded by a thermostat.

A 4-fold coincidence within a 1000 ns gate defines the trigger of the array. Using light concentrators allows to increase the array trigger rate by a factor of two. The trigger rate depends on the weather conditions and is in average to 0.8-1Hz. The trigger signal of underwater telescope is fed via more than 1km long coax cable to the center electronic station of the Cherenkov array and switched into coincidence with the array trigger signal. The time difference between them is measured by a wide range TDC. The synchronization between Cherenkov array and underwater telescope is done by comparing two underwater event counters in the central electronic station on the ice and detector electronic module of the underwater telescope read out from the shore station. The array energy threshold is about 100 TeV. The angular

resolution of the array is $\sim 0.5^\circ \div 1^\circ$ giving a good reference point to estimate the angular resolution of the underwater telescope for muons close to the vertical direction ($0^\circ \div 30^\circ$) since high energy muons retain the direction of their parent shower. In 1998 the EAS array operated in coincidence with only one string, and overall 450 events were registered. Analysis of those events showed that the accuracy of zenith angle reconstruction taking into account only time information is close to 6° , what is in reasonable agreement with MC calculations (5°). In 1999 we managed to establish the joint work of EAS array and NT-200, but unfortunately we collected only 150 events due to bad weather. The analysis of data is still in progress and results will be presented later.

2.3. Shadow of the shore in muons

Muon angular distributions as well as depth dependence of the vertical flux obtained from data taken with NT-36 have been presented earlier ²⁾. Another example which confirms the efficiency of track reconstruction uses the shore "shadow" in muons recorded with NT-96.

As it was already mentioned, NT-200 is situated at a distance of 3.6 km to the nearby shore of the lake, and more than 30 km to the opposite shore. This asymmetry allows to study the asymmetry in the azimuth distribution of muons under large zenith angles, where reconstruction for the rather "thin" NT-96 is most critical.

A sharp decrease of the muon intensity at zenith angles of $70^\circ \div 90^\circ$ is expected. The comparison of the experimental muon angular distribution with MC calculations gives us an estimation of the accuracy of the reconstruction error close to the horizontal direction.

Indeed, the NT-96 data show clear dip of the muon flux in the direction of the shore and for zenith angles larger than 70° (fig.3) – in very good agreement with calculations which take into consideration the effect of the "shadowing" shore.

3. Selected physics results

In this chapter we present some physics results based on the data of 70 days effective operating time of the 4-string array NT-96.

3.1. Separation of neutrino events with full track reconstruction

The signature of neutrino induced events is a muon crossing the detector from below. With the flux of downward muons exceeding that of upward muons from atmospheric neutrino interactions by about 6 orders of magnitude, a careful reconstruction is of prime importance. The reconstruction algorithm ²⁾ is based the assumption that the light induced by muons is emitted exactly under the Cherenkov angle (42°)

relative to the muon track. For full track reconstruction (θ , ϕ and spatial coordinates) one needs more than 5 hit channels on more than 3 strings. In contrast to first stages of the detector (NT-36 ⁸⁾), NT-96 can be considered as a real neutrino telescope for a wide region in zenith angle θ . After the reconstruction of all events with ≥ 9 hits at ≥ 3 strings (trigger 9/3), quality cuts have been applied in order to reject fake events. Furthermore, in order to guarantee a minimum lever arm for track fitting, events with a projection of the most distant channels on the track (Z_{dist}) less than 35 meters have been rejected. Due to the small transversal dimensions of NT-96, this cut excludes zenith angles close to the horizon.

The efficiency of the procedure has been tested with a sample of 1.8×10^6 MC-generated atmospheric muons, and with MC-generated upward muons due to atmospheric neutrinos. It turns out that the signal to noise ratio is > 1 for this sample.

The reconstructed angular distribution of 2×10^7 events taken with NT-96 in April/September 1996 – after all cuts – is shown in Fig.4.

From 70 days of NT-96 data, 12 neutrino candidates have been found. Nine of them have been fully reconstructed. Three nearly upward vertical tracks (see subsection 3.2) hit only 2 strings and give a clear zenith angle but ambiguities in the azimuth angle – similar to the two events from NT-36 ²⁾. This is in good agreement with MC expectations.

3.2. Search for nearly vertical upward moving neutrinos

Unlike the standard analysis ²⁾, the method presented in this section relies on the application of a series of cuts which are tailored to the response of the telescope to nearly vertically upward moving muons ^{8,9)}. The cuts remove muon events far away from the opposite zenith as well as background events which are mostly due to pair and bremsstrahlung showers below the array and to naked downward moving atmospheric muons with zenith angles close to the horizon ($\theta > 60^\circ$). The candidates identified by the cuts are afterwards fitted in order to determine the zenith angle. We included all events with ≥ 4 hits along at least one of all hit strings. To this sample, a series of 6 cuts is applied. Firstly, the time differences of hit channels along each individual string have to be compatible with a particle close to the opposite zenith(1). The event length should be large enough(2), the maximum recorded amplitude should not exceed a certain value(3), and the center of gravity of hit channels should not be close to the detector bottom(4). The latter two cuts reject efficiently brems showers from downward muons. Finally, also time differences of hits along different strings have to correspond to a nearly vertical muon (5) and the time difference between top and bottom hit in an event has to be larger than a minimum value (6).

The effective area for muons moving close to opposite zenith and fulfilling all cuts exceeds 1000 m^2 .

Within 70 days of effective data taking, 8.4×10^7 events with the muon trigger

$N_{hit} \geq 4$ have been selected.

Table 1 summarizes the number of events from all 3 event samples (MC signal and background, and experiment) which survive the subsequent cuts. After applying all cuts, four events were selected as neutrino candidates, compared to 3.5 expected from MC. One of the four events has 19 hit channels on four strings and was selected as neutrino candidate by the standard analysis too. The zenith angular distribution of these four neutrino candidates is shown in the inner box of Fig.3.

Regarding the four detected events as being due to atmospheric neutrinos, one can derive an upper limit on the flux of muons from the center of the Earth due to annihilation of neutralinos - the favored candidate for cold dark matter.

The limits on the excess muon flux obtained with underground experiments ^{10,11,12)} and NT-96 are shown in Table 2. The limits obtained with NT-96 are 4–7 times worse than the best underground limits since only the first 70 days of NT-96 have been analysed.

This result, however, illustrates the capability of underwater experiments with respect to the search for muons due to neutralino annihilation in the center of the Earth. MC shows that for NT-200 the effective area is about 2000 m², for $E_\mu > 10\text{GeV}$, two times larger than for NT-96. In case that the energy threshold for upward muons could be decreased to 5 GeV NT-200 will permit to select a non-negligible amount of contained events and estimate the energy of muons. This will allow to study the neutrino energy spectrum for neutrinos having crossed about 13000 km in the Earth ¹³⁾. Estimates show that the full number of contained events will be about 20 for $\theta > 165^\circ$ per year. In case of $\nu_\mu - \nu_x$ oscillations, the ν_μ flux will be suppressed and for $\Delta m^2 = 10^{-3}\text{eV}^2$ we will find only 7 events.

3.3. High Energy Neutrinos

The ultimate goal of large underwater neutrino telescopes is the identification of extraterrestrial high energy neutrinos. In this chapter we present results of a search for neutrinos with $E_\nu > 10\text{TeV}$ derived from NT-96 data. Cherenkov light emitted by the electro-magnetic and (or) hadronic particle cascades and high energy muons produced at the neutrino interaction vertex in a large volume around the neutrino telescope. Earlier, a similar strategy has been used by the DUMAND ¹⁴⁾ and the AMANDA ¹⁵⁾ collaborations to obtain upper limits on the diffuse flux of high energy neutrinos.

Fig.5 illustrates the detection principle. We select events with high multiplicity of hit channels corresponding to bright cascades. The volume considered for generation of cascades is essentially below the geometrical volume of NT-96 – its upper plane crosses the center of the telescope. A cut is applied which accepts only time patterns corresponding to upward traveling light signals (see below). This cut rejects most events from brems-cascades along downward muons since the majority of muons is

close to the vertical; they would cross the detector and generate a downward time pattern. Only the fewer muons with large zenith angles may escape detection and illuminate the array exclusively via bright cascades below the detector. These events then have to be rejected by a stringent multiplicity cut.

Neutrinos produce showers and high energy muons through CC-interactions

$$\nu_l(\bar{\nu}_l) + N \xrightarrow{CC} l^-(l^+) + \text{hadrons}, \quad (1)$$

through NC-interactions

$$\nu_l(\bar{\nu}_l) + N \xrightarrow{NC} \nu_l(\bar{\nu}_l) + \text{hadrons}, \quad (2)$$

where $l = e$ or μ , and through resonance production ^{16,17,18)}

$$\bar{\nu}_e + e^- \rightarrow W^- \rightarrow \text{anything}, \quad (3)$$

with the resonant neutrino energy $E_0 = M_w^2/2m_e = 6.3 \times 10^6$ GeV and cross section 5.02×10^{-31} cm².

Within the first 70 days of effective data taking, 8.4×10^7 events with the muon trigger $N_{hit} \geq 4$ have been selected.

For this analysis we used events with ≥ 4 hits along at least one of all hit strings. The time difference between any two channels deployed on the same string was required to obey the condition:

$$| (t_i - t_j) - z_{ij}/c | < a \cdot z_{ij} + 2\delta, \quad (i < j). \quad (4)$$

The t_i, t_j are the arrival times at channels i, j , and z_{ij} is their vertical distance. With $\delta = 5$ nsec accounting for the timing error, the condition $| (t_i - t_j) - z_{ij}/c | < 2\delta$ (i.e. $a = 0$) would cut for a signal traveling vertically upward with the speed of light, c . Setting a to 1 nsec/m, the acceptance cone around the opposite zenith is slightly increased. This condition has been used for almost vertically up-going muons selection earlier ^{3,19)}.

8608 events survive the selection criterion (4). Fig.6 shows the hit multiplicity distribution for these events (dashed histogram) as well as the expected one for background showers produced by atmospheric muons (solid histogram). The experimental distribution is consistent with the theoretical expectation within a factor 2. This difference can be explained by the uncertainty of the atmospheric muon flux close to horizon at the detector depth ²⁾, and by uncertainties in the dead-time of individual channels. The highest multiplicity of hit channels (one event) is $N_{hit} = 24$.

Since no events with $N_{hit} > 24$ are found in our data we can derive upper limits on the flux of high energy neutrinos which produce events with multiplicity

$$N_{hit} > 25. \quad (5)$$

The effective volume of NT-96 for neutrino induced events depends only slightly on the value of the threshold multiplicity in condition (5). For the stronger conditions $N_{hit} > 27$ and $N_{hit} > 29$, the effective volume decreases by only 11% and 27%, respectively.

The effective volume for neutrino produced events which fulfill conditions (4)-(5) was calculated as a function of neutrino energy and zenith angle θ .

The energy dependences of the effective volumes for isotropic electron and muon neutrinos are shown in Fig.7 (solid lines). Also shown are the effective volumes folded with the neutrino absorption probability in the Earth (dashed lines). The neutrino absorption in the Earth has been taken into account with suppression factor $\exp(-l(\Omega)/l_{tot})$, where $l(\Omega)$ is the neutrino path length through the Earth in direction Ω and $l_{tot}^{-1} = N_A \rho_{Earth} (\sigma_{CC} + \sigma_{NC})$ according to ^{18,20}.

3.4. The limits to the diffuse neutrino flux

The number of events due to neutrino flux Φ_ν and processes (1) and (2) is given by

$$N_\nu = T\epsilon \int d\Omega \sum_\nu \int dE V_{eff}(\Omega, E) \sum_k \int dE_\nu \Phi_\nu(E_\nu) N_A \rho_{H_2O} \frac{d\sigma_{\nu k}}{dE} \quad (6)$$

where E_ν is the neutrino energy and E - the energy transferred to a shower or high energy muon. The index ν indicates the summation over neutrino types ($\nu = \nu_\mu, \bar{\nu}_\mu, \nu_e$) and k over CC and NC interactions. N_A is the Avogadro number, $\epsilon = 0.9$ - the detector efficiency. Cross sections from R.Gandhi *et al.*(1996) have been used.

The shape of the neutrino spectrum was assumed to behave like E^{-2} as typically expected for Fermi acceleration. In this case, 90% of expected events would be produced by neutrinos from the energy range $10^4 \div 10^7$ GeV with the center of gravity around 2×10^5 GeV. Comparing the calculated rates with the upper limit to the actual number of events, 2.3 for 90% CL, and assuming the flavor ratios $\Phi_{\nu_\mu} = \Phi_{\bar{\nu}_\mu} = \Phi_{\nu_e}$ due to photo-meson production of π^+ followed by the decay $\pi^+ \rightarrow \mu^+ + \nu_\mu \rightarrow e^+ + \nu_e + \bar{\nu}_\mu + \nu_\mu$ for extraterrestrial sources ^{21,22}, we obtain the following upper limit to the diffuse neutrino flux:

$$\frac{d\Phi_\nu}{dE} E^2 < 1.43 \times 10^{-5} \text{cm}^{-2} \text{s}^{-1} \text{sr}^{-1} \text{GeV}. \quad (7)$$

New theoretical upper bounds to the intensity of high-energy neutrinos from extraterrestrial sources have been presented recently ^{21,22}. These upper bounds as well as our limit and limits obtained by DUMAND ¹⁴), AMANDA ¹⁵), EAS-TOP ²³) and FREJUS ²⁴) experiments are shown in Fig.8. Also, the atmospheric neutrino fluxes ²⁵) from horizontal and vertical directions (upper and lower curves, respectively) are presented.

For resonant process (3) the event number is given by:

$$N_{\bar{\nu}_e} = T\epsilon \int d\Omega \int dE V_{eff}(\Omega, E) \int_{(M_w - 2\Gamma_w)^2/2m_e}^{(M_w + 2\Gamma_w)^2/2m_e} dE_\nu \Phi_{\bar{\nu}_e}(E_\nu) \frac{10}{18} N_A \rho_{H_2O} \frac{d\sigma_{\bar{\nu}_e, e}}{dE} \quad (8)$$

$$M_w = 80.22\text{GeV}, \quad \Gamma_w = 2.08\text{GeV}.$$

Our 90% CL limit at the W resonance energy is:

$$\frac{d\Phi_{\bar{\nu}}}{dE_{\bar{\nu}}} \leq 3.6 \times 10^{-18} \text{cm}^{-2} \text{s}^{-1} \text{sr}^{-1} \text{GeV}^{-1}. \quad (9)$$

This limit lies between limits obtained by DUMAND ($1.1 \times 10^{-18} \text{cm}^{-2} \text{s}^{-1} \text{sr}^{-1} \text{GeV}^{-1}$) and EAS-TOP ($7.6 \times 10^{-18} \text{cm}^{-2} \text{s}^{-1} \text{sr}^{-1} \text{GeV}^{-1}$).

The new limits (10) and (12) have been obtained with the underwater detector NT-96. We hope that the analysis of 3 years data taking with NT-200^{3,19)} will allow us to lower this limit substantially.

3.5. Search for Fast Monopoles ($\beta > 0.75$)

Fast bare monopoles with unit magnetic Dirac charge and velocities greater than the Cherenkov threshold in water ($\beta = v/c > 0.75$) are promising survey objects for underwater neutrino telescopes. For a given velocity β the monopole Cherenkov radiation exceeds that of a relativistic muon by a factor $(gn/e)^2 = 8.3 \times 10^3$ ($n = 1.33$ - index of refraction for water)^{26,27)}. Therefore fast monopoles with $\beta \geq 0.8$ can be detected up to distances 55 m \div 85 m which corresponds to effective areas of $(1-3) \times 10^4 \text{m}^2$.

The natural way for fast monopole detection is based on the selection of events with high multiplicity of hits. In order to reduce the background from downward atmospheric muons we restrict ourself to monopoles coming from the lower hemisphere.

Two independent approaches have been used for selection of upward monopole candidates from the 70 days of NT-96 data. The first one is similar to the method which was applied to upward moving muons (see subsection 3.2), with an additional cut $N_{hit} > 25$ on the hit multiplicity. The second one cuts on the value of space-time correlation, followed by a cut $N_{hit} > 35$ on the hit multiplicity. The upper limits on the monopole flux obtained with the two different methods coincide within errors.

The same type of analysis was applied to the data taken during 0.42 years lifetime with the neutrino telescope NT-36²⁸⁾.

The combined 90% C.L. upper limit obtained by the Baikal experiment for an isotropic flux of bare fast magnetic monopoles is shown in Fig.9, together with the best

limits from underground experiments Soudan2, KGF, MACRO and Ohya^{29,30,31,32}).

4. Limnology

Besides physics goals NT-200 can be used as a powerful tool to monitor water parameters. The array permanently records phototubes counting rates, and periodically parameters like optical transmission at various wavelengths, temperature, conductivity, pressure, and sound velocity. All these data complement traditional limnological studies are of importance to get a comprehensive understanding of processes occurring in the lake. Just for illustration we show OMs counting rate variations at various time scales recorded with NT-36 in 1993/94. Counting rates of individual OMs as well as individual channels (coincidence rate of a pair OMs) are dominated by water luminescence. Fig.10 presents the counting rate over 2 years and compares it to the bacteria concentration measured at distance of 50 km to the NT-200 site, at 10 m depth below surface. In August/September we observe an increase of the luminosity to extremely high levels. The changes of the counting rate of channels are not reflected in the muon trigger rate, since the muon trigger is dominated by atmospheric muons, with negligible contribution by random hits (water luminescence or dark current pulses). This is demonstrated in fig.11 on a shorter time scale, for a time interval of marked changes of individual channel counting rates following a severe storm at August 3rd, 1993, which had washed a lot of water from a nearby rivers and crooks to the lake. Fig.12 shows a short period of about 8 hours when the counting rates sequentially increased, starting with highest OMs and ending with the lowest ones along the string. From the time shift of the 3 curves a vertical current of $2.3 \text{ cm}\cdot\text{s}^{-1}$ is deduced. This is remarkable since the vertical velocity of water renewal is considered to be most intensively, is only $0.2 \div 0.3 \text{ cm}\cdot\text{s}^{-1}$.

5. Conclusions and Outlook

The results obtained with intermediate detector stages show the capability of Baikal Neutrino Telescope to search for the wide variety of phenomena in neutrino astrophysics, cosmic ray physics and particle physics.

The first atmospheric neutrinos have been identified. Also limits on the fluxes of magnetic monopoles, diffuse flux of very high energy neutrinos as well as of neutrinos from WIMP annihilation in the center of the Earth have been derived.

In the following years, NT-200 will be operated as a neutrino telescope with an effective area between 1000 and 5000 m^2 , depending on the energy, and will investigate atmospheric neutrino spectra above 10 GeV.

NT-200 can be used to search for neutrinos from WIMP annihilation and for magnetic monopoles and high energy extraterrestrial neutrinos. It will also be a unique environmental laboratory to study water processes in Lake Baikal.

Apart from its own goals, NT-200 is regarded to be a prototype for the development a large scale telescope of next generation with an effective area of several 10^4 m². The basic design of such a detector is under discussion at present.

This work was supported by the Russian Ministry of Research, the German Ministry of Education and Research and the Russian Fund of Fundamental Research (grants 99-02-18373a, 97-02-17935, 99-02-31006k, 97-02-96589 and 97-05-96466).

REFERENCES

- 1) *The Baikal Neutrino Telescope NT-200, BAIKAL 92-03* (1992)
- 2) I.A.Belolaptikov *et al.*, *Astroparticle Physics* **7** (1997) 263.
- 3) I.A.Belolaptikov *et al.*, *astro-ph/9903341* (1999) (accepted for publ. in *Astropart. Phys.*).
- 4) R.I.Bagduev *et al.*, *Nucl. Instr. Meth.* **A420** (1999) 138 ÷ 154.
- 5) R.I.Bagduev *et al.*, *Proc. Int. Conference on Trends in Astroparticle Physics*, 132 (Aachen, 1994)
- 6) L.B.Bezrukov *et al.*, *Proc. 3rd NESTOR Workshop, Oct. 1993, Greece*, 645 ÷ 657.
- 7) R.A.Antonov *et al.*, *Proc. 23-rd ICRC Calgary*, vol.2 (1993) 430 ÷ 433
- 8) L.B.Bezrukov *et al.*, *Proc. of the 2nd Workshop on the Dark Side of the Universe*, 221 (Rome, 1995) (astro-ph/9601161)
- 9) V.A.Balkanov *et al.* 1998 *Preprint INR 0972/98* (in russian)
- 10) M.M.Boliev *et al.* *Nucl.Phys.* (Proc. Suppl.) **48** (1996) 83
- 11) T.Montaruli *et al.* *Proc. 25-th ICRC Durban–South Africa*, vol.7, (1997) 185
- 12) M.Mori *et al.* *Phys. Rev.* **D48** (1993) 5505
- 13) L.Moscoso Oral presentation at NOW98 1998.
- 14) J.W.Bolesta *et al.* *Proc. 25-th ICRC Durban–South Africa*, vol.7, (1997) 29
- 15) R.Porrata *et al.* *Proc. 25-th ICRC Durban–South Africa*, vol.7, (1997) 9
- 16) S.L.Glashow, *Phys. Rev.* bf 118 (1960) 316
- 17) V.S.Beresinsky and A.Z.Gazizov, *JETP Lett.* **25** (1977) 254
- 18) R.Gandhi *et al.* *Astroparticle Physics* **5** (1996) 81
- 19) V.A.Balkanov *et al.*, *Physics of Atomic Nuclei* **62** (1999) 949
- 20) V.S.Berezinsky *et al.*, *Sov. J. Nucl. Phys.* **43** (1986) 406
- 21) E.Waxman, and J.Bahcall, *Phys. Rev.* **D 59** (1999) 023002; E.Waxman, and J.Bahcall, *Phys. Rev. Lett.* **78** (1997) 2292
- 22) R.J.Protheroe *e-preprint astro-ph/9809144* (1998)
- 23) M.Aglietta *et al.* *Phys. Lett.* **B333** (1994) 555
- 24) W.Rhode *et al.*, *Astropart. Phys.* **4** (1994) 217
- 25) P.Lipari, *Astropart. Phys.* **1** (1993) 195

- 26) I.M.Frank 1988 *Vavilov-Cherenkov Radiation* (Moscow: Nauka) 192 (in russian)
- 27) D.A.Kirzhnits and V.V.Losjakov *Pis'ma Zh. Eksp.Theor.Fz.* **42** (1985) 226
- 28) V.A.Balkanov *et al.* Preprint INR (Moscow: INR) (1998) (in russian)
- 29) S.Orito *et al.* *Phys. Rev. Lett.* **66** (1992) 1951.
- 30) M.Ambrosio *et al.* *MACRO Preprint* MACRO/PUB 98/3 (1998)
- 31) H.Adarkar *et al.* *Proc. 21st ICRC. Adelaide.* (1990) 95
- 32) J.L.Thorn *et al.* *Phys. Rev.* **D46** (1992) 4846

Table 1. The expected number of atmospheric neutrino events and background events, and the observed number of events after cuts 1–6.

after cut $N^\circ \rightarrow$	1	2	3	4	5	6
atm. ν , MC	11.2	5.5	4.9	4.1	3.8	3.5
background, MC	7106	56	41	16	1.1	0.2
experiment	8608	87	66	28	5	4

Table 2. 90% C.L. upper limits on the muon flux from the center of the Earth for four regions of zenith angles obtained in different experiments

Zenith angles	Flux limit ($10^{-14} \cdot (cm^2 sec)^{-1}$)			
	NT-96 > 10GeV	<i>Baksan</i> > 1GeV	<i>MACRO</i> > 1.5GeV	<i>Kam-de</i> > 3GeV
$\geq 150^\circ$	11.0	2.1	2.67	4.0
$\geq 155^\circ$	9.3	3.2	2.14	4.8
$\geq 160^\circ$	5.9 – 7.7	2.4	1.72	3.4
$\geq 165^\circ$	4.8	1.6	1.44	3.3

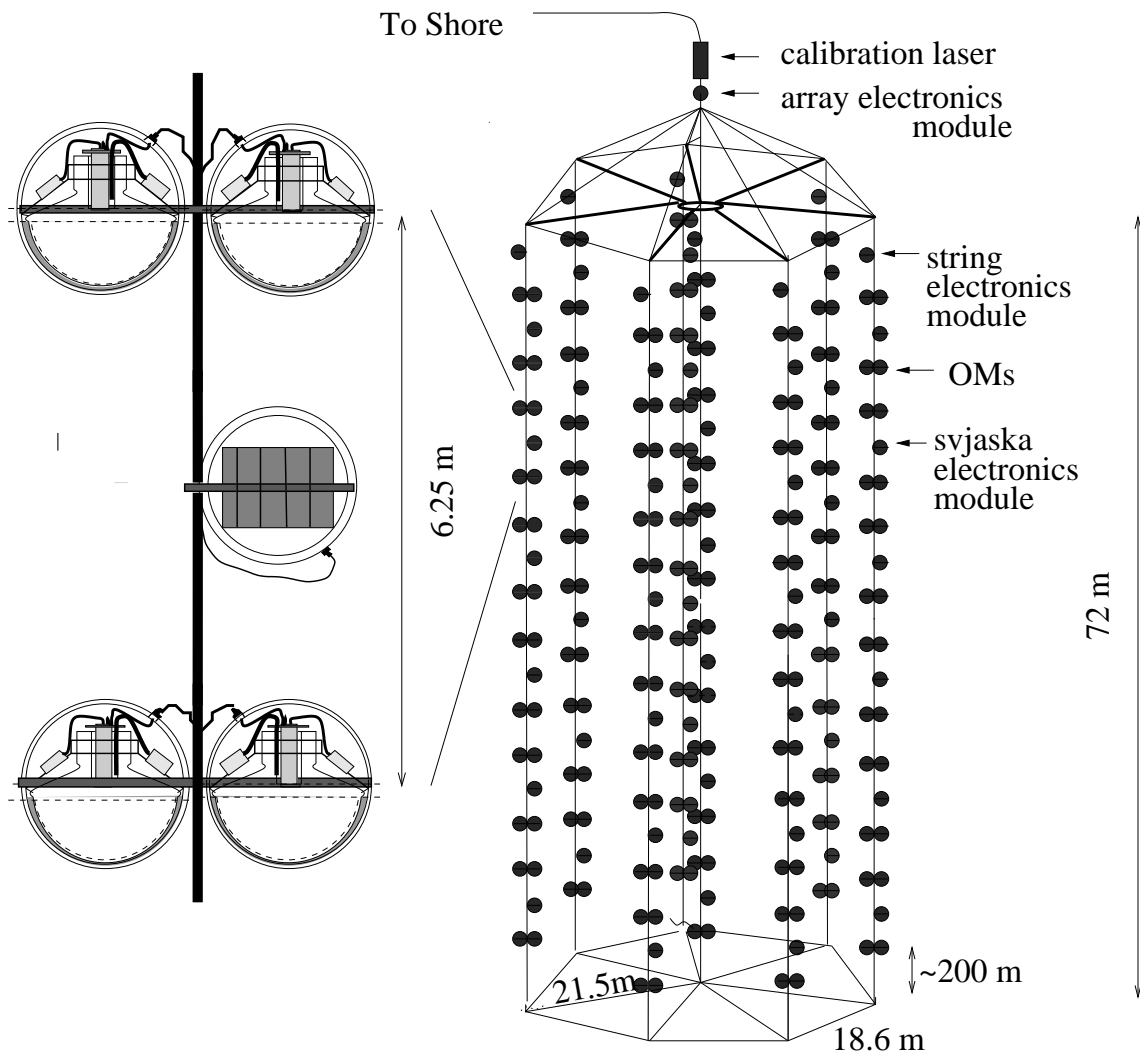


Fig. 1. Schematic view of the Baikal Telescope NT-200. The array is time-calibrated by two nitrogen lasers. The one (fiber laser) is mounted just above the array. Its light is guided via optical fibers to each OM pair. The other (water laser) is arranged 20 m below the array. Its light propagates directly through the water. The expansion left-hand shows 2 pairs of optical modules (“svjaska”) with the svjaska electronics module, which houses parts of the read-out and control electronics.

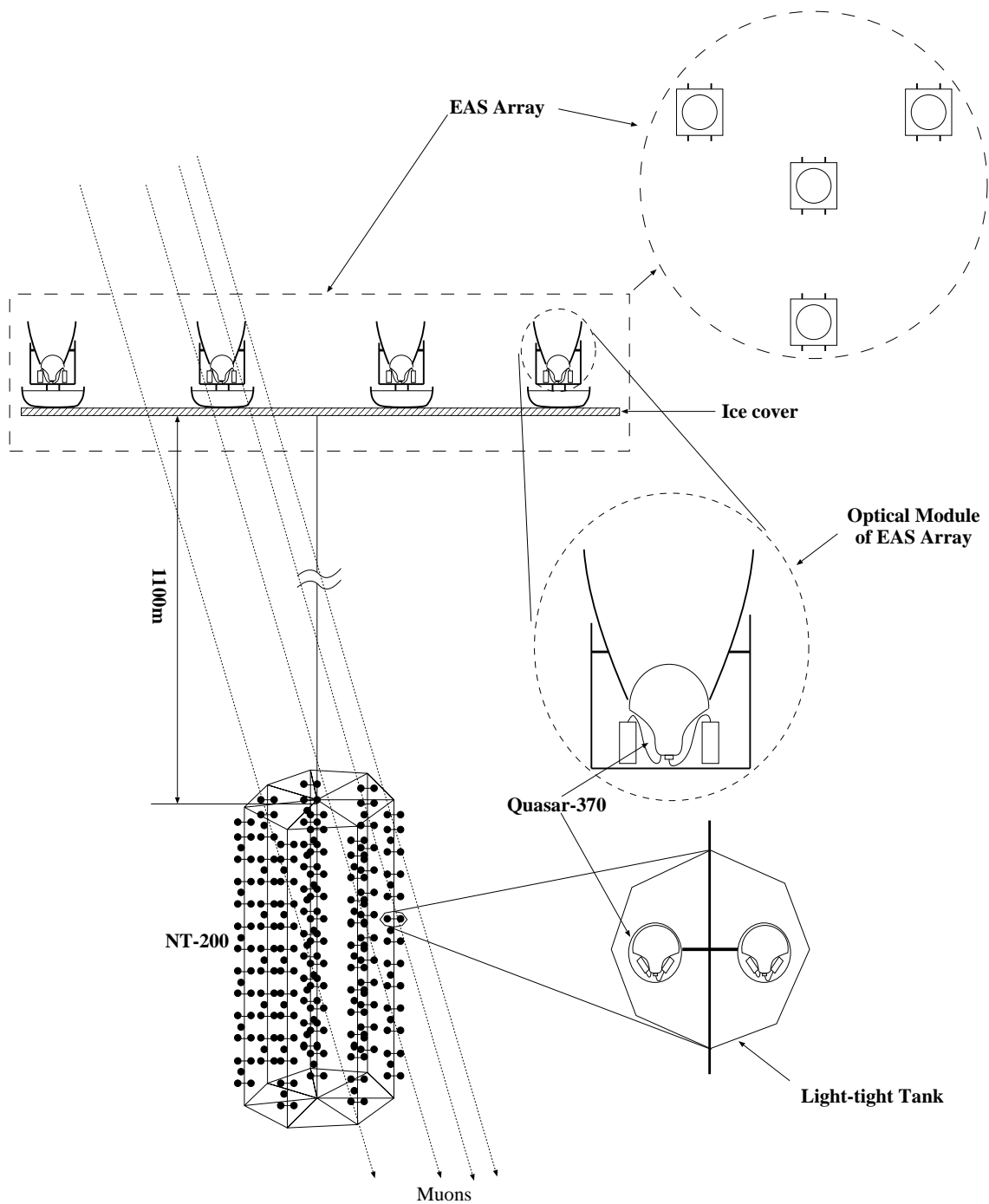


Fig. 2. The principle of joint operation of NT-200 with an EAS Cherenkov array. Also shown (bottom right) are optical modules contained in a light tight tank. Their signal fixes one track point as a tool for calibration.

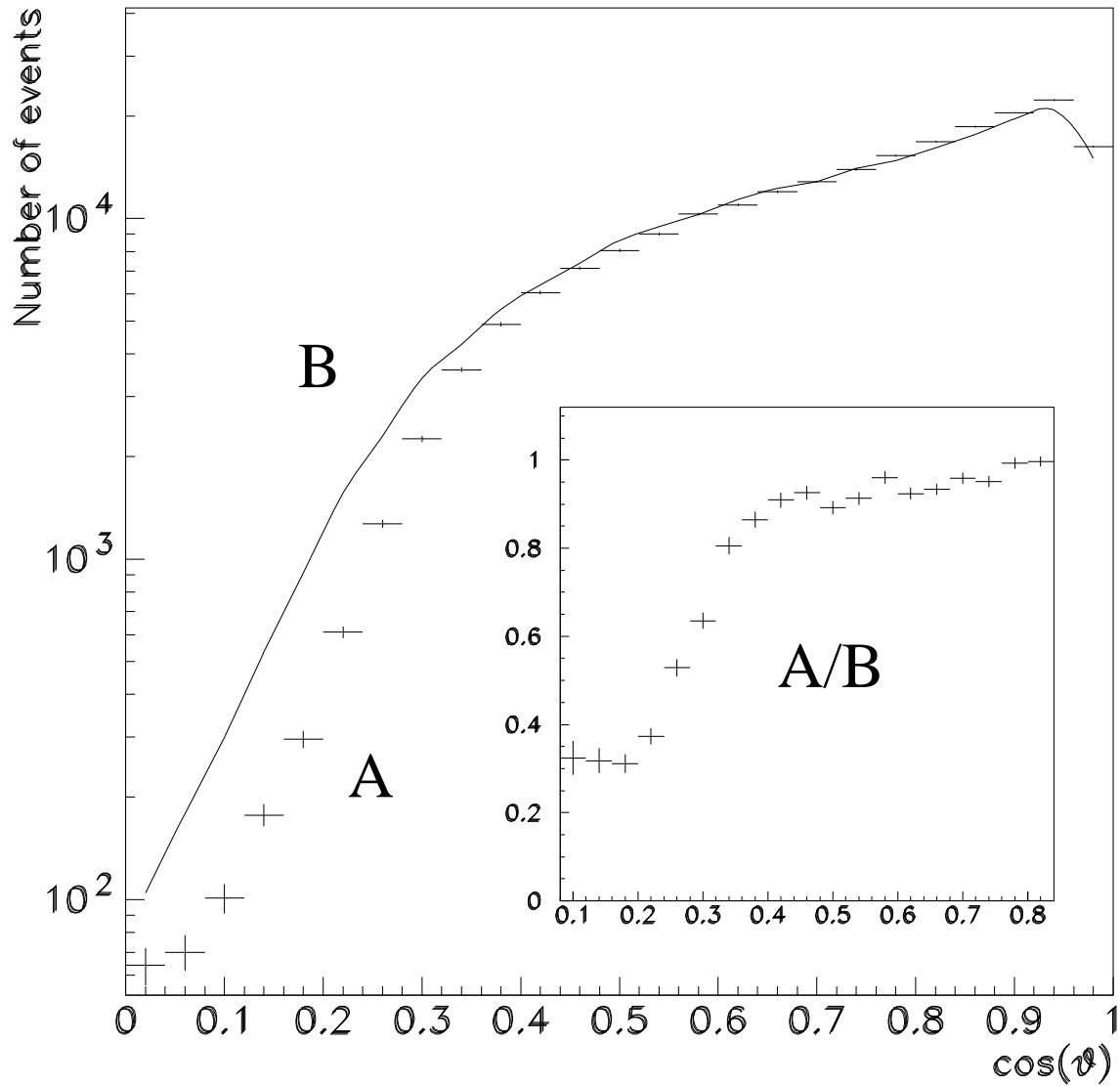


Fig. 3. Atmospheric muons (vs zenith angle θ) as it is measured in the direction to the nearest point of the shore(A) and in the opposite direction (B) - “open” water. The small picture shows the ratio A to B.

70 days Baikal NT-96

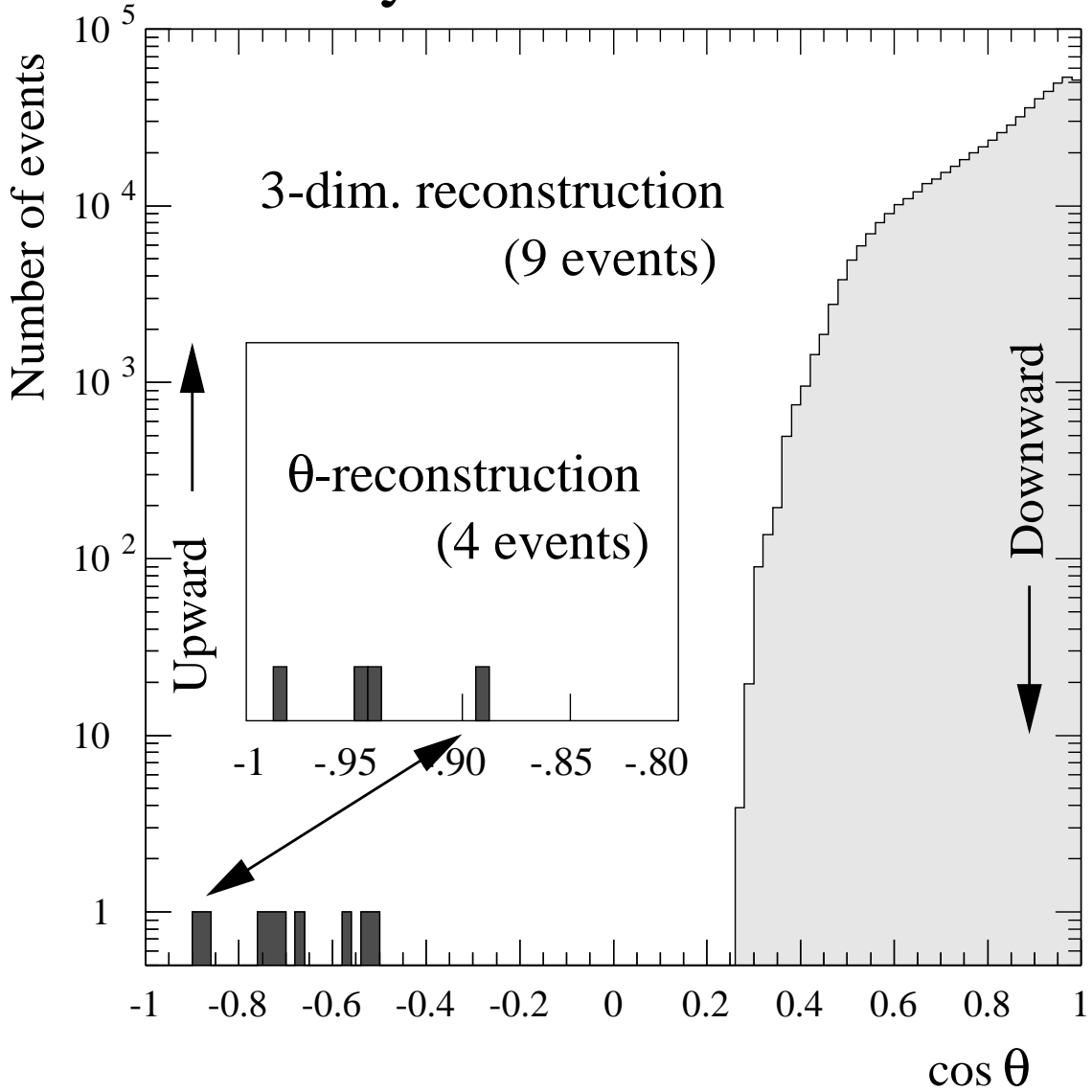


Fig. 4. Experimental angular distribution of events satisfying trigger $9/3$, all final quality cuts and the limit on Z_{dist} (see text). The small picture shows the events selected by using the method described in subsection 3.1. The event found by both algorithms is marked by the arrow.

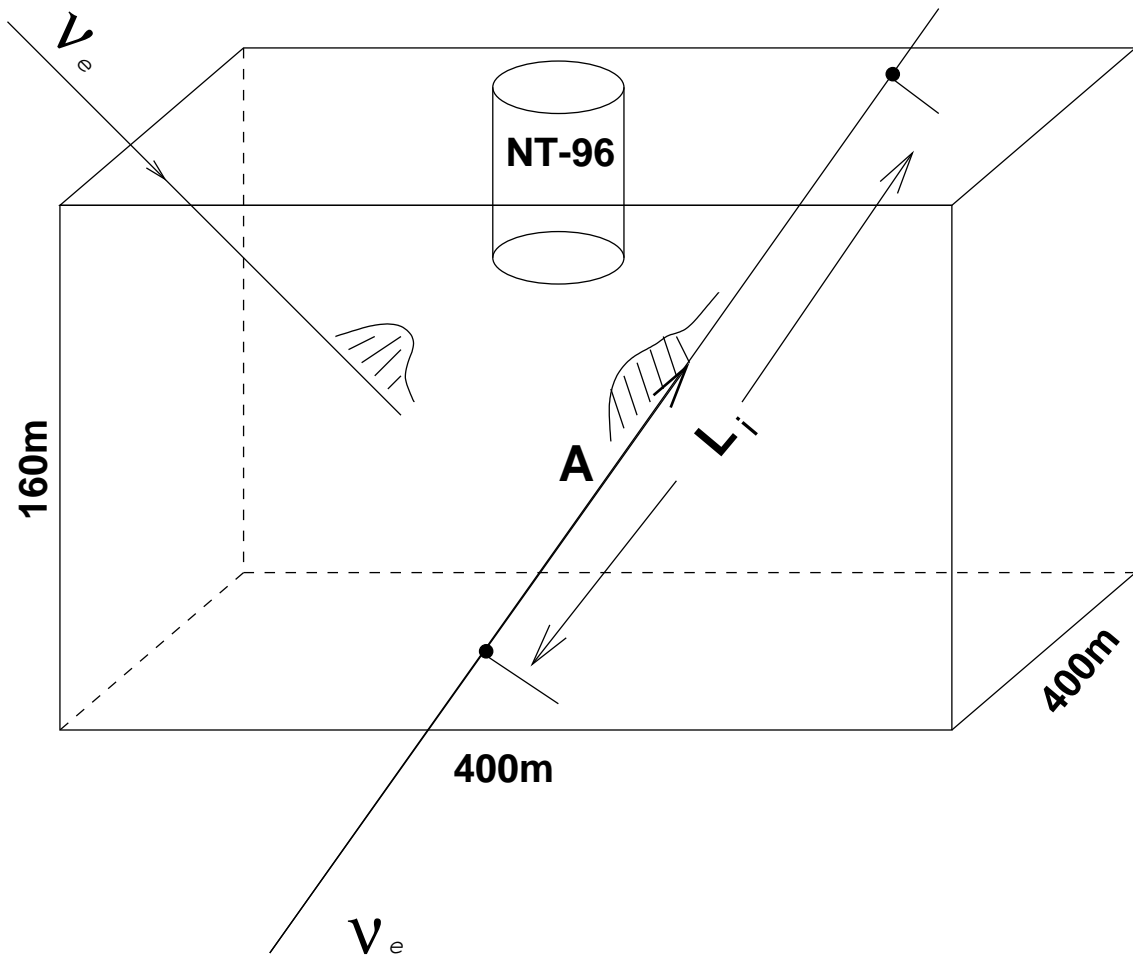


Fig. 5. Detection principle for neutrino induced showers with NT-96.

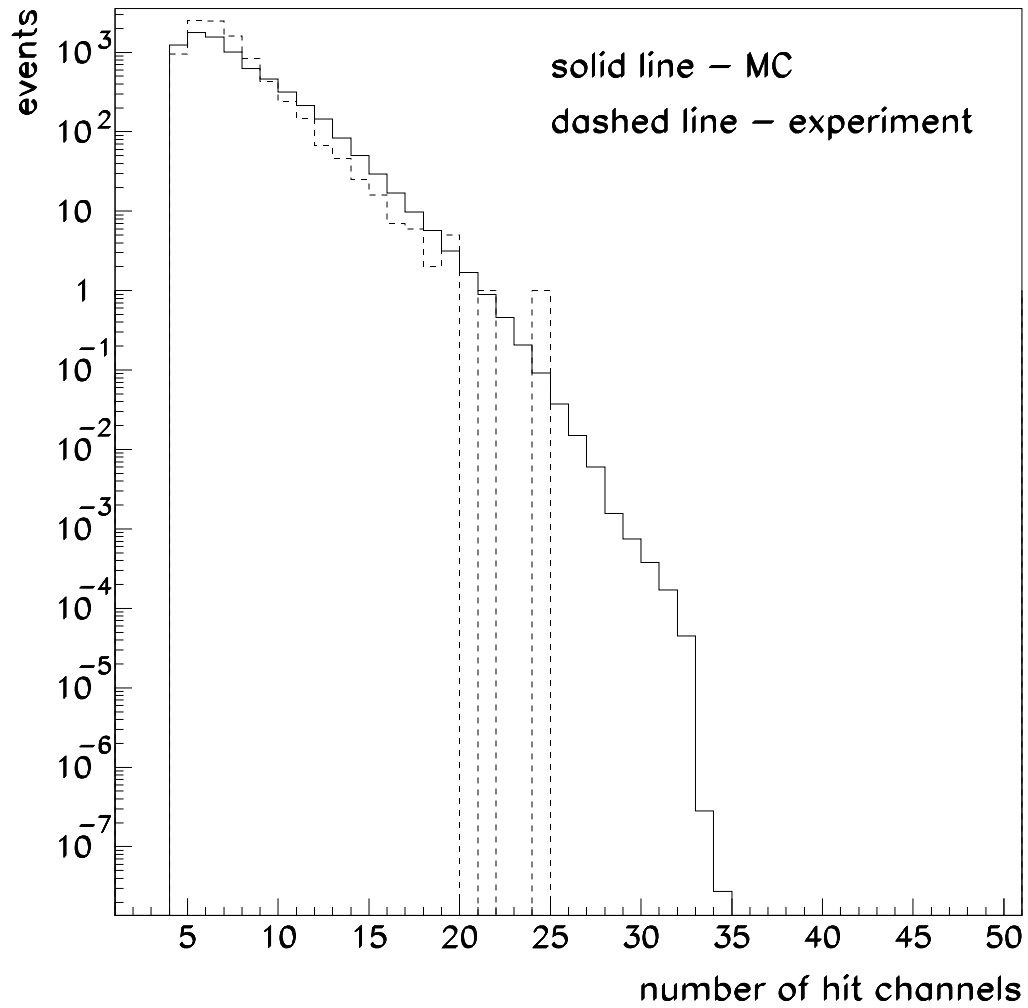


Fig. 6. Hit channel multiplicity: solid histogram - showers produced by atmospheric muons (MC), dashed histogram - experiment.

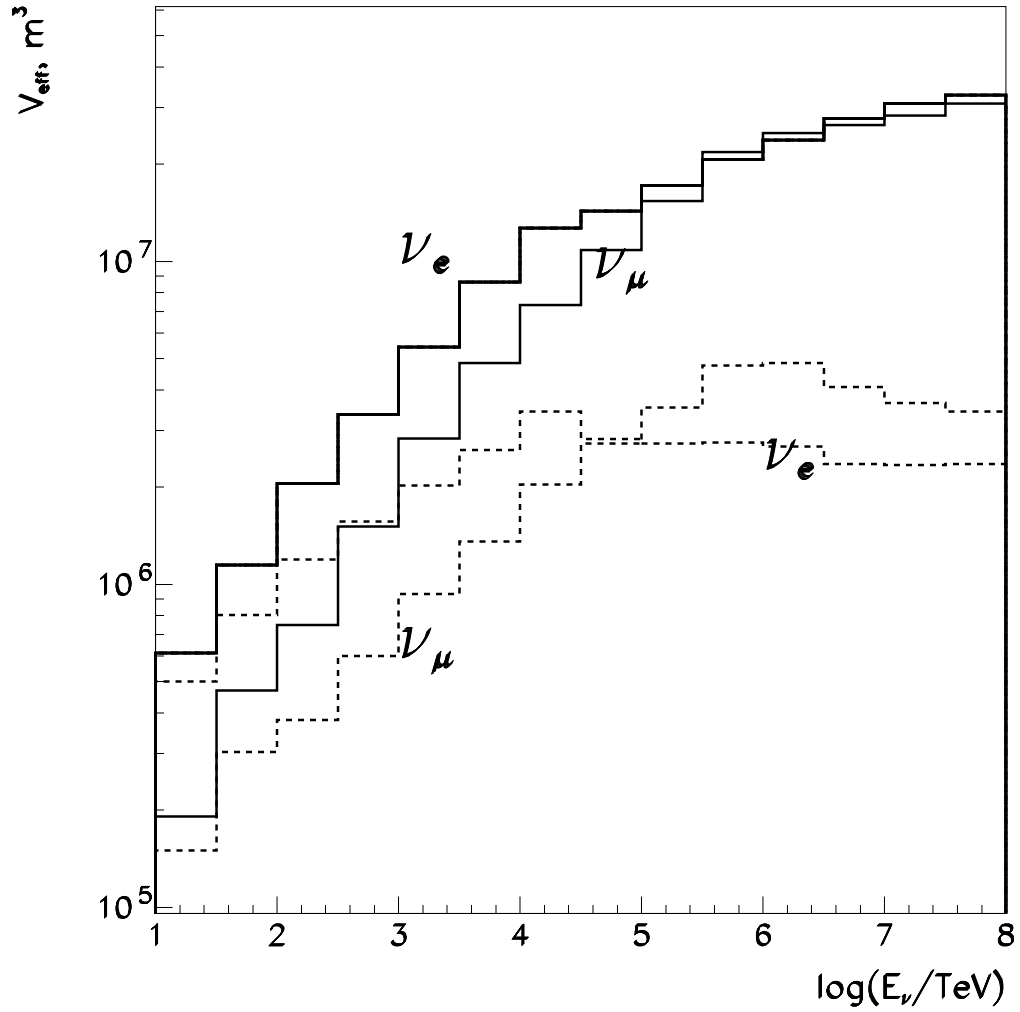


Fig. 7. Effective volumes of NT-96 for isotropic electron and muon neutrinos (solid lines). The dashed lines represent the effective volumes folded with the neutrino absorption probability in the Earth (see text).

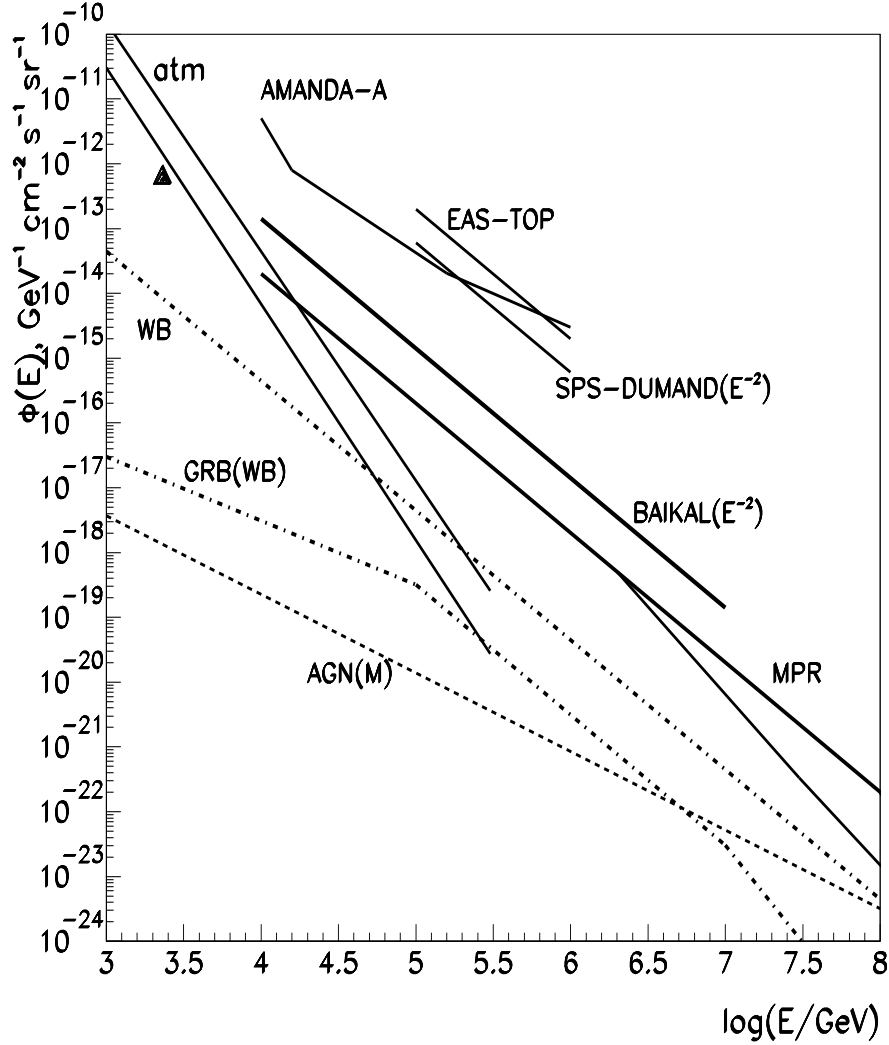


Fig. 8. Upper limits to the differential flux of high energy neutrinos obtained by different experiments as well as upper bounds for neutrino fluxes from a number of different models. Dot-dash curves labeled WB and GRB(WB) - upper bound and neutrino intensity from GRB estimated by Waxman and Bahcall (1997,1999); dashed curve labeled AGN(M) - neutrino intensity from AGN (Mannheim model A, 1996); solid curves labeled MPR - upper bounds for $\nu_\mu + \bar{\nu}_\mu$ in Mannheim et al. (1998) for pion photo-production neutrino sources with different optical depth τ (adapted from ref.17). The triangle denotes the limit obtained by the Frejus-Experiment for an energy of 2.6 TeV : $7 \times 10^{-13} \text{cm}^{-2} \text{s}^{-1} \text{sr}^{-1} \text{GeV}^{-1}$.

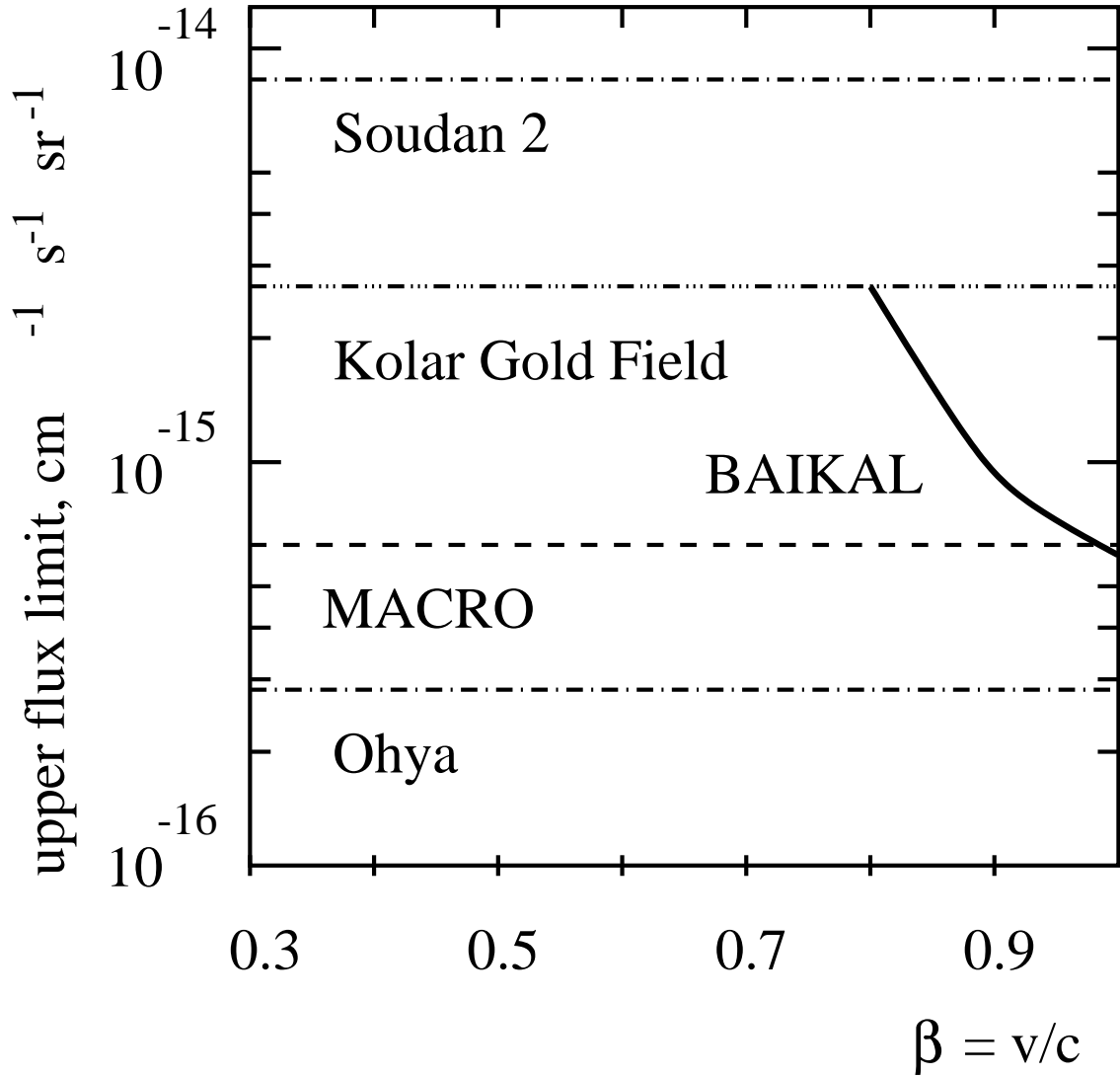


Fig. 9. The 90% C.L. Baikal upper limit for an isotropic flux of bare magnetic monopoles compared with other published limits.

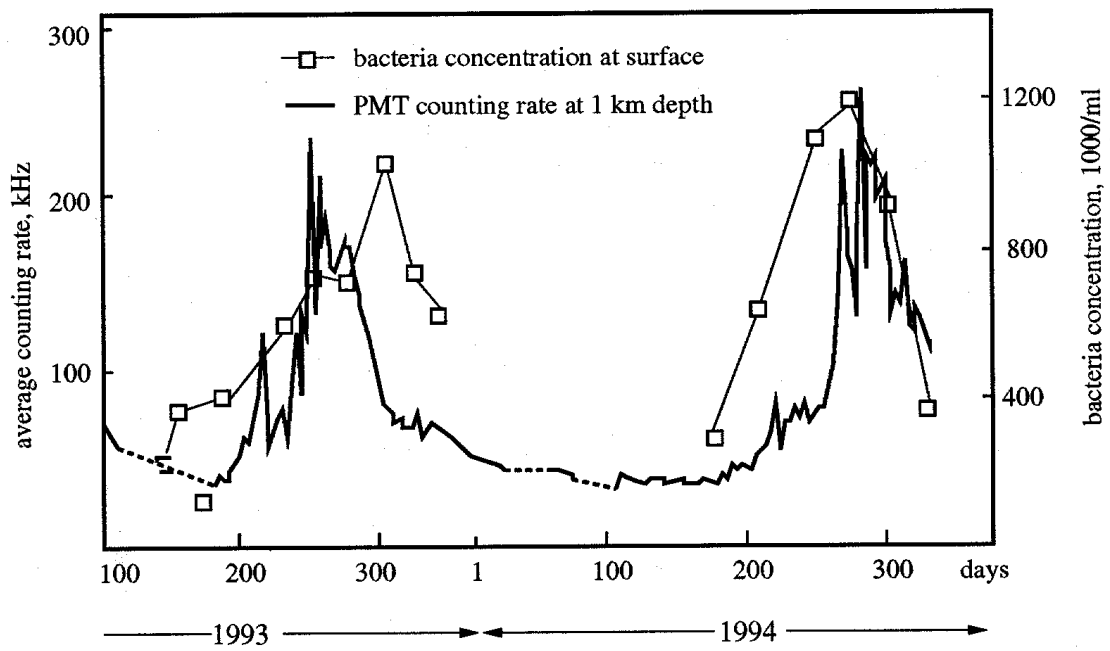


Fig. 10. Average counting rate of OMs vs. time, compared to bacteria concentration at surface.

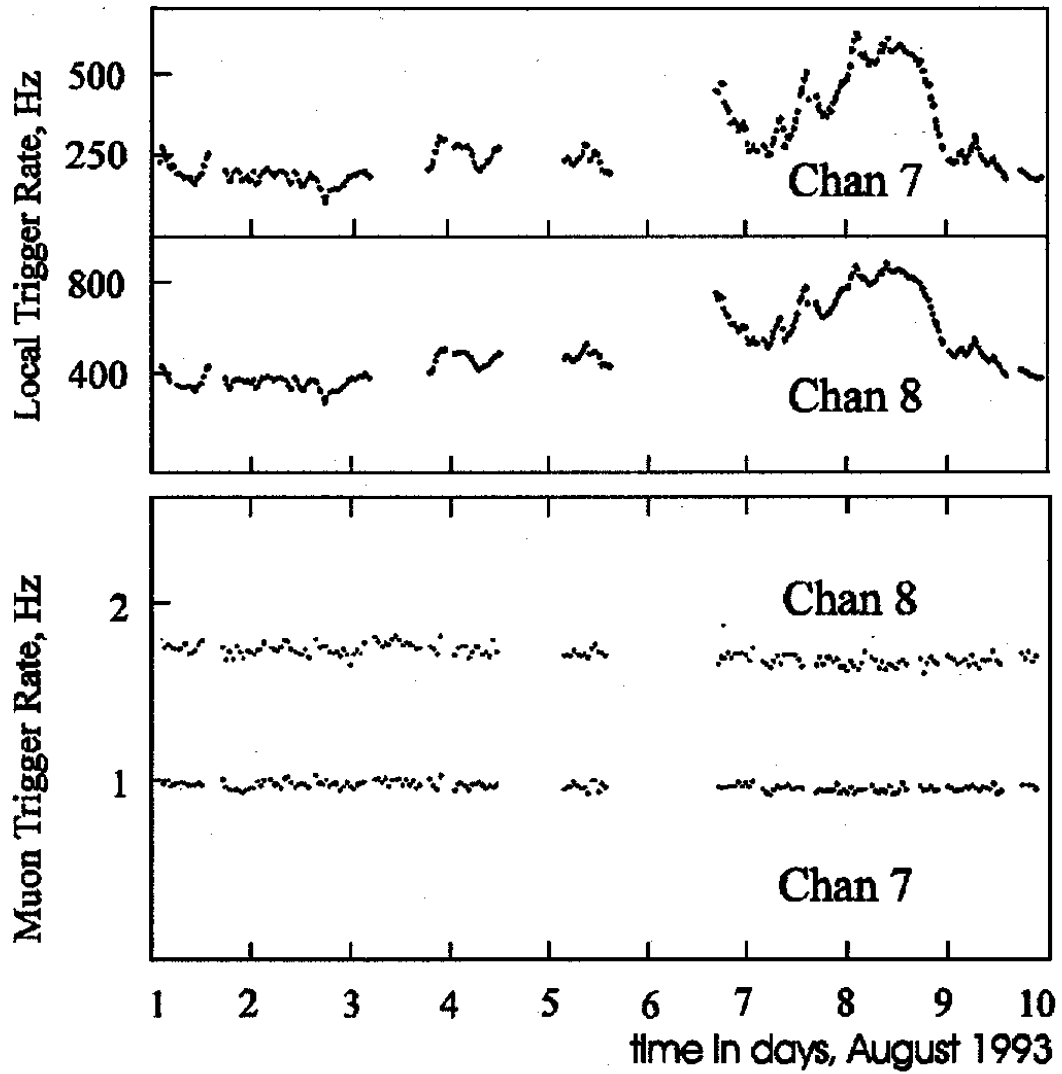


Fig. 11. a) Local trigger rates for channel 7 (downward facing) and channel 8 (upward facing) for August 1st-9th, 1993. The counting rates are averaged over 30 min. b) Muons trigger rates (condition 4/1) for channel 7 and 8. Counting rates are averaged over 50 min.

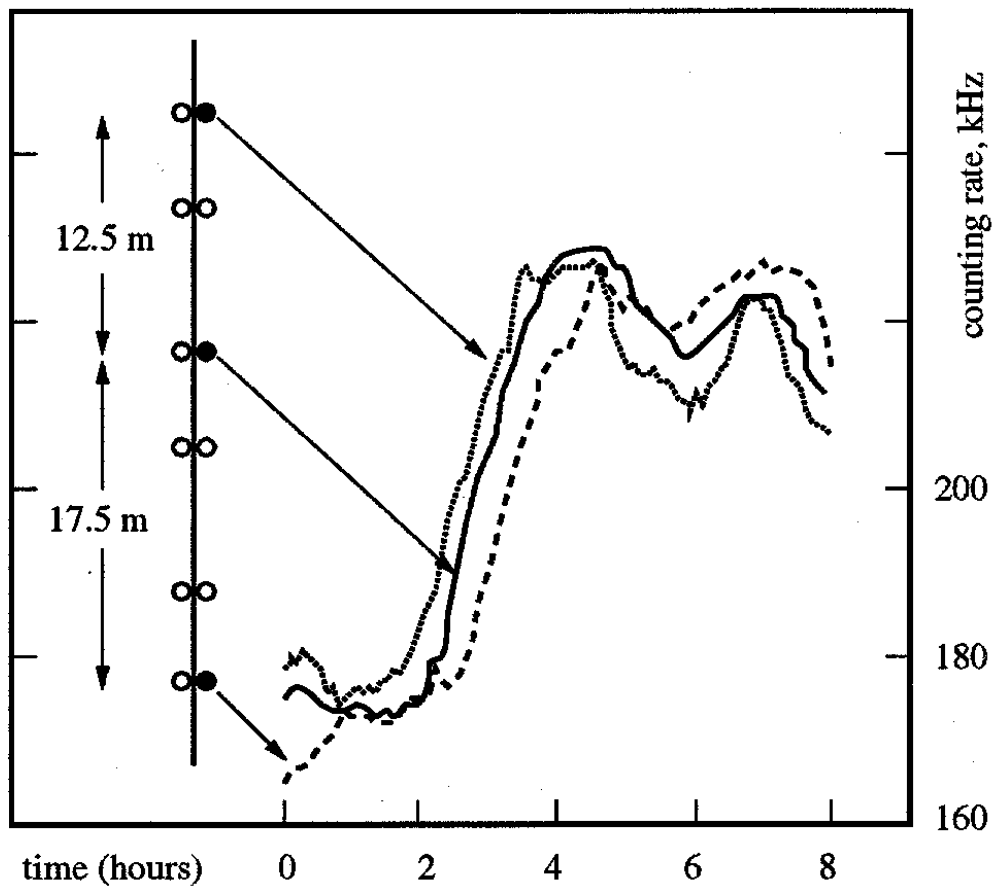


Fig. 12. Counting rate of three OMs along one string during an 8 hour interval at Sept. 24, 1993.